ELSEVIER

Physica C 295 (1998) 93–100

PHYSICA C

The Cooper pair dispersion relation

M. Casas [a], S. Fujita [b], M. de Llano [c,*], A. Puente [a], A. Rigo [a], M.A. Solís [d]

[a] *Departament de Física, Universitat de les Illes Balears, 07071 Palma de Mallorca, Spain*
[b] *Department of Physics, SUNY, Buffalo, NY 14260-1500, USA*
[c] *Instituto de Investigaciones en Materiales, UNAM, 04510 México DF, México*
[d] *Instituto de Física, UNAM, 01000 México DF, México*

Received 26 August 1997; accepted 22 September 1997

Abstract

The binding energy of a Cooper pair formed with the BCS model interaction potential is obtained numerically for all coupling in two and three dimensions for all non-zero center-of-mass momentum (CMM) of the pair. The pair breaks up for very small CMM, at most about four orders of magnitude smaller than the maximum CMM allowed by the BCS model interaction, and its binding energy is remarkably linear over the entire range of the CMM up to breakup. © 1998 Elsevier Science B.V.

PACS: 03.65.G; 71.10.Li; 05.30.Fk
Keywords: Phonon mechanism; Electron–phonon coupling; Pair breaking

1. Introduction

Pairing of fermions in superconductivity theories is commonly considered to be only among partners of equal and opposite linear momenta, i.e., into pairs with zero net center-of-mass momentum (CMM). We investigate non-zero CMM pairing, and in particular the dependence on the CMM of the pair binding energy, mentioned in Schrieffer's [1] monograph on superconductivity as being linear in the long wavelength (small CMM) limit, in contrast to the expected [2] quadratic behaviour of a particle moving freely in vacuum. In this paper we first review the derivation of the Cooper pair eigenvalue equation for the pair binding energy as a function of its CMM. Next, this equation is reduced in two and three dimensions to double-integral equations that are solvable analytically for small CMM and numerically for arbitrary CMM. Finally, Cooper pairs are distinguished and compared with several familiar ''collective modes''.

* Corresponding author. Tel.: +52 11 525 6224631; fax: +52 11 525 6161251.

PII S0921-4534(97)01740-1

2. Non-zero center-of-mass momentum pairing

Besides the rest energy, the total energy E_K of a (Cooper) pair [3] of fermions of momentum $\hbar\boldsymbol{k}_1$ and $\hbar\boldsymbol{k}_2$ and with center-of-mass momentum (CMM) $\hbar\boldsymbol{K}$ interacting pairwise and immersed in a background of $N-2$ inert spectator fermions in a spherical Fermi surface (in k-space) of radius k_F is obtained as follows. Let the relative and center-of-mass coordinates be $\boldsymbol{r}\equiv\boldsymbol{r}_1-\boldsymbol{r}_2$ and $\boldsymbol{R}\equiv\frac{1}{2}(\boldsymbol{r}_1+\boldsymbol{r}_2)$, respectively. The corresponding wave vectors are related through

$$\boldsymbol{K}=\boldsymbol{k}_1+\boldsymbol{k}_2,\quad \boldsymbol{k}=\tfrac{1}{2}(\boldsymbol{k}_1-\boldsymbol{k}_2). \tag{1}$$

Define the kinetic energy operators

$$\hat{T}_i=-\frac{\hbar^2}{2m^*}\nabla_i^2;\quad \hat{T}_1+\hat{T}_2=\hat{T}_r+\hat{T}_R=-\frac{\hbar^2}{m^*}\nabla_r^2-\frac{\hbar^2}{4m^*}\nabla_R^2, \tag{2}$$

with m^* the effective fermion mass. The eigenvalue equation for the total energy E_K is then

$$\left(\hat{T}_r+\hat{T}_R+\hat{V}_K\right)\Psi_K=E_K\Psi_K, \tag{3}$$

where

$$\Psi_K=\psi(\boldsymbol{r})\Phi_K(\boldsymbol{R}), \tag{4}$$

$$\Phi_K(\boldsymbol{R})=\mathrm{e}^{\mathrm{i}\boldsymbol{K}\cdot\boldsymbol{R}} \tag{5}$$

and

$$\hat{V}_K\Psi_K=\int \mathrm{d}\boldsymbol{r}'\,V_K(\boldsymbol{r},\boldsymbol{r}')\psi(\boldsymbol{r}')\Phi_K(\boldsymbol{R}), \tag{6}$$

with $V_K(\boldsymbol{r},\boldsymbol{r}')$ a general non-local pair interaction. Expanding $\psi(\boldsymbol{r})$ in a complete set of plane-wave states,

$$\psi(\boldsymbol{r})=\sum_{\boldsymbol{k}} C_{\boldsymbol{k}}\mathrm{e}^{\mathrm{i}\boldsymbol{k}\cdot\boldsymbol{r}} \tag{7}$$

the Cooper problem consists in setting

$$C_{\boldsymbol{k}}=0\quad \text{for all } k_1,\ k_2<k_F \text{ or } |\boldsymbol{k}\pm\tfrac{1}{2}\boldsymbol{K}|<k_F. \tag{8}$$

It is this restriction that distinguishes Cooper's from Schrödinger's equation, which is for two particles in vacuum while the Cooper problem refers to two particles in a medium of $N-2$ other fermions satisfying the Pauli Exclusion Principle. Combining Eqs. (2)–(8) gives

$$\sum_{\boldsymbol{k}}\left[\left(\frac{\hbar^2}{m^*}k^2+\frac{\hbar^2}{4m^*}K^2\right)\mathrm{e}^{\mathrm{i}\boldsymbol{k}\cdot\boldsymbol{r}}+\int \mathrm{d}\boldsymbol{r}'\,V_K(\boldsymbol{r},\boldsymbol{r}')\mathrm{e}^{\mathrm{i}\boldsymbol{k}\cdot\boldsymbol{r}'}-E_K\mathrm{e}^{\mathrm{i}\boldsymbol{k}\cdot\boldsymbol{r}}\right]C_{\boldsymbol{k}}\mathrm{e}^{\mathrm{i}\boldsymbol{K}\cdot\boldsymbol{R}}=0. \tag{9}$$

Putting $\epsilon_l\equiv\hbar^2l^2/2m^*$, multiplying Eq. (9) by $\mathrm{e}^{-\mathrm{i}\boldsymbol{k}'\cdot\boldsymbol{r}}$, integrating over $\boldsymbol{r}$, using $\int \mathrm{d}\boldsymbol{r}\exp(\mathrm{i}\boldsymbol{Q}\cdot\boldsymbol{r})=L^d\delta_{\boldsymbol{Q},0}$ where L^{d} is the system volume in d dimensions, and cancelling the $\mathrm{e}^{\mathrm{i}\boldsymbol{k}\cdot\boldsymbol{R}}$, leaves

$$\left(2\epsilon_{k'}+\tfrac{1}{2}\epsilon_K\right)C_{\boldsymbol{k}'}+\sum_{\boldsymbol{k}}V^K_{\boldsymbol{k},\boldsymbol{k}'}C_{\boldsymbol{k}}=E_KC_{\boldsymbol{k}'} \tag{10}$$

where

$$V^K_{\boldsymbol{k},\boldsymbol{k}'}\equiv\frac{1}{L^d}\int \mathrm{d}\boldsymbol{r}\int \mathrm{d}\boldsymbol{r}'\,\mathrm{e}^{-\mathrm{i}\boldsymbol{k}'\cdot\boldsymbol{r}}V_K(\boldsymbol{r},\boldsymbol{r}')\mathrm{e}^{\mathrm{i}\boldsymbol{k}\cdot\boldsymbol{r}'}. \tag{11}$$

The *BCS model interaction* to be used here assumes that

$$V^K_{\boldsymbol{k},\boldsymbol{k}'} = \begin{cases} -V\theta\left(2\sqrt{k_F^2+k_D^2}-K\right) & \text{if } k_F < |\boldsymbol{k}\pm\tfrac{1}{2}\boldsymbol{K}|,\ |\boldsymbol{k}'\pm\tfrac{1}{2}\boldsymbol{K}| < \sqrt{k_F^2+k_D^2} \\ 0 & \text{otherwise} \end{cases} \tag{12}$$

with $V>0$, and $\hbar\omega_D \equiv \hbar^2 k_D^2/2m^*$ the maximum energy of a vibrating ionic lattice phonon. The step function reflects the fact that the interaction operates only if $0 \le K \le 2\sqrt{k_F^2+k_D^2}$. This means that two fermions interact with a constant attraction $-V$ when the tip of their relative momentum wavevector $\boldsymbol{k}$ points anywhere inside the overlap volume in k-space of the two spherical shells in Fig. 1. Using Eq. (12), Eq. (10) simplifies to

$$\left(2\epsilon_k - E_K + \hbar^2K^2/4m^*\right)C_{\boldsymbol{k}} = V\theta\left(2\sqrt{k_F^2+k_D^2}-K\right)\sum_{\boldsymbol{k}'}{}' C_{\boldsymbol{k}'} \equiv -A_K \tag{13}$$

with the prime on the summation sign denoting the restrictions over $\boldsymbol{k}$ in Eq. (12). Solving for $C_{\boldsymbol{k}}$ leads to

$$C_{\boldsymbol{k}} = \frac{-A_K}{2\epsilon_k - E_K + \hbar^2K^2/4m^*}. \tag{14}$$

Multiplying this by $V\theta(2\sqrt{k_F^2+k_D^2}-K)$ and summing over $\boldsymbol{k}$, restricted as in Eq. (12), gives

$$1 = V\theta\left(2\sqrt{k_F^2+k_D^2}-K\right)\sum_{\boldsymbol{k}}{}'\left(2\epsilon_k - E_K + \hbar^2K^2/4m^*\right)^{-1}. \tag{15}$$

Setting the total energy eigenvalue $E_K \equiv 2E_F - \Delta_K$, the pair is bound if $\Delta_K > 0$ and Eq. (15) becomes an eigenvalue equation for the pair (positive) binding energy Δ_K. For $K=0$ it becomes

$$1 = V\sum_{\boldsymbol{k}}{}'\left(2\epsilon_k - 2E_F + \Delta_0\right)^{-1} = V\int_{E_F}^{E_F+\hbar\omega_D}\frac{g(\epsilon)\,d\epsilon}{2\epsilon - 2E_F + \Delta_0} \tag{16}$$

from which one immediately obtains the familiar result

$$\Delta_0 = \frac{2\hbar\omega_D}{e^{2/\lambda}-1} \underset{\lambda\to 0}{\to} 2\hbar\omega_D e^{-2/\lambda} \tag{17}$$

for the $K=0$ pair binding energy, where $\lambda \equiv g(E_F)V$ is a dimensionless coupling constant and $g(E_F)$ is the density of (fermionic) states for each spin evaluated at the Fermi surface. The equality in Eq. (17) is exact in 2D for all coupling—as well as in 1D or 3D provided that $\hbar\omega_D \ll E_F$ so that $g(\epsilon) \approx g(E_F)$, a constant that can be taken outside the integral in Eq. (16).

Note that since Eq. (17) yields only $\Delta_0 \le 11$ K (for $\lambda \le 1/2$ and $\Theta_D \approx 300$ K) compared with the total rest mass energy of two electrons which is $\sim 10^{10}$ K, a Cooper pair is very weakly bound indeed when compared, say, with the deuteron for which these two energies are, respectively, about 2 and 2000 MeV, or with the pi-meson as made up of a ''down'' and ''up'' quark where the two energies are, respectively 560 and 700 MeV.

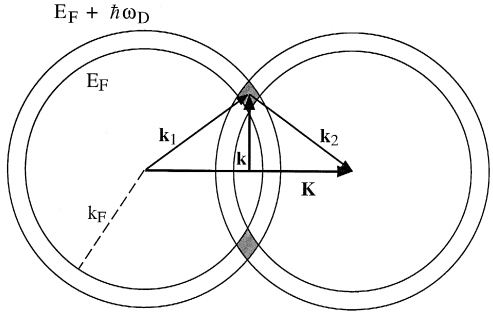

Fig. 1. Cross-section of overlap volume in k-space (shading) where the tip of the relative wave vector $\boldsymbol{k}$ must point for the attractive BCS model interaction Eq. (12) to be non-zero, for a Cooper pair of CMM $\hbar\boldsymbol{K}$.

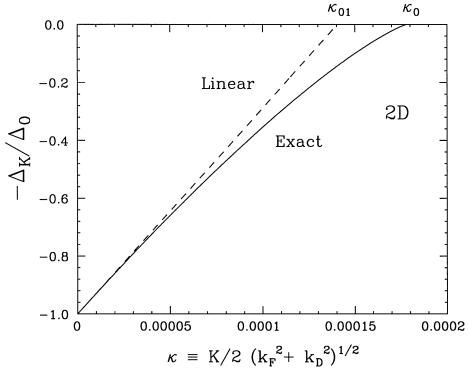

Fig. 2. Exact 2D Cooper pair dispersion relation calculated numerically from Eq. (18) for $\lambda = 0.5$ and $\nu = 10^{-2}$, compared with its linear approximation Eq. (19).

For a two-dimensional system Eq. (15) reduces (see Appendix A) to

$$1 = \frac{4\lambda}{\pi}\int_0^{\pi/2} d\phi \int_{[1-\kappa^2(1+\nu)\sin^2\phi]^{1/2}+\kappa(1+\nu)^{1/2}\cos\phi}^{[1+\nu-\kappa^2(1+\nu)\sin^2\phi]^{1/2}-\kappa(1+\nu)^{1/2}\cos\phi} d\xi\,\xi\left(\tilde{\Delta}_\kappa + 2(1+\nu)\kappa^2 - 2 + 2\xi^2\right)^{-1}, \tag{18}$$

where $g(E_F) \equiv L^2 m^*/2\pi\hbar^2$ the 2D density of states; $\xi \equiv k/k_F$; $\kappa \equiv K/2(k_F^2 + k_D^2)^{1/2}$; $\tilde{\Delta}_\kappa \equiv \Delta_K/E_F$; and $\nu \equiv \hbar\omega_D/E_F = k_D^2/k_F^2$. For small K, one obtains analytically from Eq. (18)

$$\Delta_K \underset{K\to 0}{\to} \Delta_0 - \frac{2}{\pi}\frac{\left[(1+\nu)^{1/2} + e^{2/\lambda}\right]}{e^{2/\lambda} - 1}\hbar v_F K + O(K^2) \tag{19}$$

which for weak coupling $\lambda \to 0$ reduces to

$$\Delta_K \underset{K\to 0}{\to} \Delta_0 - \frac{2}{\pi}\hbar v_F K + O(K^2). \tag{20}$$

Fig. 2 compares Δ_K in the linear approximation Eq. (19) to the exact dispersion relation obtained numerically from Eq. (18), for $\lambda = 0.5$ and $\nu = 10^{-2}$. Indeed, the linear approximation is very good for moderately small λ and ν over the entire range of K values for which $\Delta_K \geq 0$. Pair breakup, specifically $\Delta_K < 0$, occurs at a relative small value of K, about four orders of magnitude smaller than the maximum value $2\sqrt{k_F^2 + k_D^2}$ allowed by the interaction Eq. (12) for the values of λ and ν exhibited in the figures.

In three dimensions, assuming $\nu \ll 1$ and the 3D density of states $g(\varepsilon) = (L^3/\pi^2\hbar^3)\sqrt{m^{*3}\varepsilon/2} \approx g(E_F)$, Eq. (15) becomes (see Appendix A)

$$1 = 2\lambda\int_0^{\pi/2} d\phi \sin\phi \int_{[1-\kappa^2(1+\nu)\sin^2\phi]^{1/2}+\kappa(1+\nu)^{1/2}\cos\phi}^{[1+\nu-\kappa^2(1+\nu)\sin^2\phi]^{1/2}-\kappa(1+\nu)^{1/2}\cos\phi} d\xi\,\xi^2\left[\tilde{\Delta}_\kappa + 2(1+\nu)\kappa^2 - 2 + 2\xi^2\right]^{-1} \tag{21}$$

which for small K, assuming from Eq. (17) the weak coupling expression $\tilde{\Delta}_0 \approx 2\nu e^{-2/\lambda}$ which is very accurate for the typical range of λ and ν values (see Fig. 4 below), gives

$$\Delta_K \underset{K\to 0}{\to} \Delta_0 - e^{4/\lambda}\frac{\sqrt{1-\nu e^{-2/\lambda}}\,(2e^{-2/\lambda} + \nu e^{-2/\lambda} + 1)}{e^{2/\lambda}\nu\{\ln A + \ln B\} + \nu\ln(AB) + 2e^{2/\lambda}\sqrt{1-\nu e^{-2/\lambda}}} \times \frac{1}{\left(e^{2/\lambda} + 1 - \sqrt{1+\nu}\right)}\hbar v_F K + O(K^2), \tag{22}$$

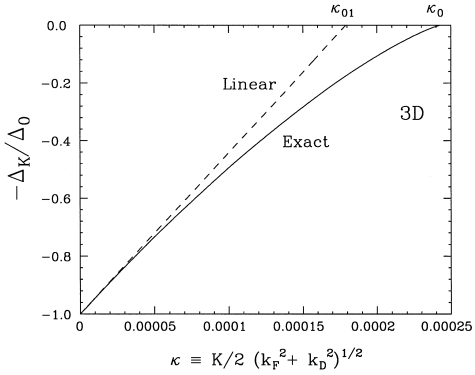

Fig. 3. Exact 3D Cooper pair dispersion relation calculated numerically from Eq. (21) for $\lambda = 0.5$ and $\nu = 10^{-2}$, compared with its linear approximation Eq. (22).

where $A \equiv (\sqrt{1+\nu} - \sqrt{1-\nu e^{-2/\lambda}})/(\sqrt{1+\nu} + \sqrt{1-\nu e^{-2/\lambda}})$, and $B \equiv (1+\sqrt{1-\nu e^{-2/\lambda}})/(1-\sqrt{1-\nu e^{-2/\lambda}})$. For $\nu \ll 1$, $\lambda \to 0$ and $K \to 0$, Eq. (22) reduces to the result cited in Ref. [1], namely

$$\Delta_K \underset{K\to 0}{\to} \Delta_0 - \tfrac{1}{2}\hbar v_F K + O(K^2). \tag{23}$$

Results in 3D are qualitatively similar to those in 2D and are illustrated in Fig. 3.

In Fig. 4 are compared the weak coupling asymptotic Cooper pair binding energy in Eq. (17) to the exact value Δ_0 for a range of ν values and for several λ values. In 2D, Δ_0 is given exactly by the equality in Eq. (17), while for 3D it was obtained numerically by solving Eq. (21), with $\kappa = 0$. The two are seen to agree very well for small λ for the relevant empirical values of $\nu \approx 10^{-3}$ in 3D, at least for conventional (elemental) superconductors, and for all ν in 2D.

3. Collective modes in a superconductor

Collective modes in a superconductor have indeed been discussed since the late 1950s by Nambu, Anderson, Rickayzen, and Bardasis and Schrieffer. A review of the early work by Martin is available [6], as is a more

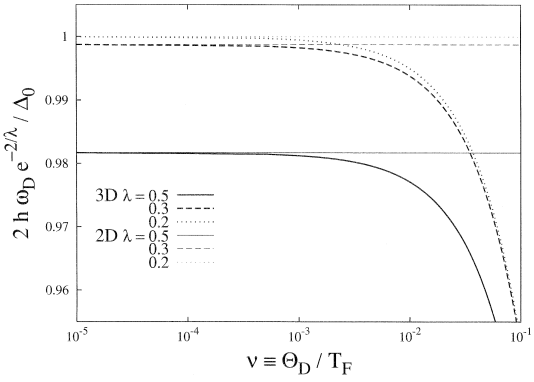

Fig. 4. Fractional deviation of the weak coupling asymptotic value $2\hbar\omega_D e^{-2/\lambda}$ in Eq. (17) of the zero-CMM Cooper pair binding energy, to its exact value Δ_0, as function of $\nu \approx \Theta_D / T_F$ for three values of λ, in both 2D (thin straight lines) and 3D (thick curves). In 2D the exact Δ_0 is given by the equality in Eq. (17) for any ν. In 3D Δ_0 must be obtained numerically from Eq. (21) with $\kappa = 0$. For 2D-like cuprate superconductors ν is empirically [4] 0.03 to 0.07; for 3D-like conventional (elemental) superconductors $\nu \approx 10^{-3}$.

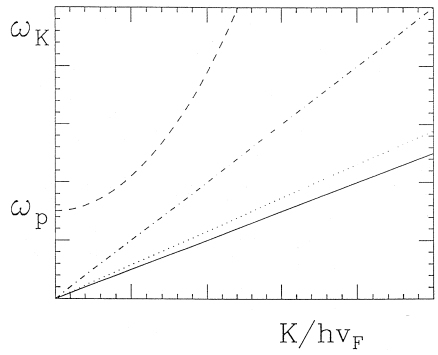

Fig. 5. Dispersion curves for: the plasmon Eq. (24) (dashed); the weak coupling (repulsive interaction) zero-sound phonon Eq. (25) (dot-dashed); the weak coupling (attractive interaction) Anderson mode Eq. (28) (dotted); and the weak coupling 3D Cooper pair dispersion $\Delta_0 - \Delta_K$ from Eq. (23) (full curve).

recent treatment by Belkhir and Randeria [7]. However, we do not deal here with ''collective modes'' but rather with (non-zero center-of-mass) ''Cooper pairs'' which can Bose–Einstein condense while collective modes cannot. Cooper pairs are *entities distinct* from collective modes such as zero-sound phonons or plasmons since they: (a) are bounded in number (before the thermodynamic limit is taken), and (b) are fixed in number as they carry a fixed constituent fermion number (namely two), while phonons or plasmons, say, do not share either property. Fig. 5 compares and contrasts them in the long wavelength limit ($K \to 0$). The dashed quadratic curve is the plasmon dispersion relation (see Ref. [5], p. 180), for an electron gas

$$\omega_K = \omega_P \left[1 + \tfrac{9}{10}(K/K_{TF})^2 + \ldots\right] \tag{24}$$

in the ''ring (RPA) approximation'' valid for $r_s \equiv r_0/a_0 \equiv [(4\pi/3)n)]^{-1/3}/(\hbar^2/me^2) \ll 1$, where r_0 is an average electron spacing, $n \equiv k_F^3/3\pi^2$ being the electron number density, a_0 the first Bohr radius $\hbar^2/me^2$ with m the electron mass, while the plasmon frequency is $\omega_P \equiv \sqrt{4\pi ne^2/m}$ and the ''Thomas–Fermi inverse screening length'' is $K_{TF} \equiv \sqrt{6\pi ne^2/E_F}$ with $E_F \equiv \hbar^2 k_F^2/2m$ as before. The dot-dashed curve is the weak coupling zero-sound phonon dispersion (Ref. [5], p. 183), curve for repulsive interactions between fermions at $T = 0$, and is given by

$$\omega_K \simeq \left[1 + 2\exp\left\{-\left[2\pi^2\hbar^2/mk_F\,\nu(0) + 2\right]\right\}\right] v_F K \tag{25}$$

for $\nu(0) \ll \hbar^2/mk_F$, where $\nu(\boldsymbol{q}) \equiv \int d^3r\, e^{-i\boldsymbol{q}\cdot\boldsymbol{r}} V(\boldsymbol{r})$ and $V(\boldsymbol{r})$ the (repulsive) interparticle interaction potential. The slope of this straight line rises as coupling is increased, and assumes the form

$$\omega_K \simeq \left[\nu(0)/3\pi^2\left(\hbar^2/mk_F\right)\right]^{1/2} v_F K \tag{26}$$

for $\nu(0) \gg \hbar^2/mk_F$. Note that Eq. (26) can be rewritten as

$$\omega_K^2 \simeq \frac{\nu(0)}{3\pi^2\left(\hbar^2/mk_F\right)} v_F^2 K^2 \tag{27}$$

and becomes the plasmon frequency squared ω_P^2 if $\nu(K)$ is taken as the Fourier integral of the Coulomb interaction, $4\pi e^2/K^2$. On the other hand, for attractive interactions $V < 0$ between the fermions one has the so-called ''Anderson mode'' [6],

$$\omega_K \simeq \left[1 - 4g(E_F)|V|\right] \frac{1}{\sqrt{3}} v_F K \tag{28}$$

in the weak coupling limit, which is shown as the dotted curve in Fig. 5. Finally, the weak coupling Cooper pair dispersion relation $\Delta_0 - \Delta_K$ from Eq. (23) is represented by the full curve. In 2D, the Anderson mode Eq. (28)

carries [7] a factor $1/\sqrt{2}$ instead of the $1/\sqrt{3}$ of 3D; it thus also lies higher than the 2D Cooper pair dispersion relation Eq. (20) since $1/\sqrt{2} > 2/\pi$.

Of possible interest is that the quadratic correction term in Eq. (19) just after the linear term diverges exponentially like $e^{2/\lambda}$ in the limit of zero coupling, as was verified by computer-algebra expansion of Δ_K in powers of K in 2D. This suggests that Eq. (19) does not possess a power expansion in K beyond and including the K^2 term for all coupling. An analogous divergence, though much weaker, also occurs with the plasmon dispersion relation Eq. (24), rewritten explicitly as

$$\omega_K = \omega_P\left(1 + \frac{9\pi}{40}\frac{\hbar^2}{m^* e^2 k_F}K^2 + \ldots\right) \tag{29}$$

in the limit of weak coupling $e^2 \to 0$.

4. Conclusions

The Cooper pair binding energy for the BCS model interaction acting pairwise between fermions decreases almost linearly to zero with the pair center-of-mass momentum (CMM) as was determined numerically for all coupling from the Cooper eigenvalue equation in both two and three dimensions. This linear behaviour contrasts with the quadratic dispersion relation of a bound composite particle moving in vacuum, e.g., a deuteron.

Acknowledgements

M.C. and M. de Ll. acknowledge partial support from grant PB95-0492 and SAB95-0312 (Spain). M. de Ll. and M.A. S. acknowledge partial support from UNAM-DGAPA-PAPIIT-IN103894 (México). M. de Ll. thanks R.M. Carter, N.J. Davidson, D.M. Eagles and O. Rojo for extensive discussions and/or correspondence, and NATO (Belgium) for a research grant.

Appendix A

We sketch the derivation of working Eq. (18) in 2D and Eq. (21) in 3D, from the Cooper pair eigenvalue Eq. (15). Since $E_K \equiv 2E_F - \Delta_K$, the latter equation can be written in d-dimensions as

$$1 = V\left(\frac{L}{2\pi}\right)^d \int' \frac{\mathrm{d}\boldsymbol{k}}{\hbar^2\left(k^2 - k_F^2\right)/m^* + \Delta_K + \hbar^2 K^2/4m^*} \tag{A.1}$$

where the prime on the integral sign again denotes the restrictions in Eq. (12). These restrictions are identical in two and three dimensions, and can be written as

$$k_F^2 < |\boldsymbol{k} - \tfrac{1}{2}\boldsymbol{K}|^2 = k^2 - kK\cos\phi + \tfrac{1}{4}K^2, \tag{A.2}$$

$$k_F^2 + k_D^2 > |\boldsymbol{k} + \tfrac{1}{2}\boldsymbol{K}|^2 = k^2 + kK\cos\phi + \tfrac{1}{4}K^2 \tag{A.3}$$

with ϕ the angle between $\boldsymbol{k}$ and $\boldsymbol{K}$, since it can be limited to values between 0 and $\pi/2$ because of symmetry. Manipulating Eqs. (A.2) and (A.3) we obtain

$$k^2 - kK\cos\phi + \tfrac{1}{4}K^2 - k_F^2 > 0, \tag{A.4}$$

$$k^2 + kK\cos\phi + \tfrac{1}{4}K^2 - k_F^2 - k_D^2 < 0. \tag{A.5}$$

These conditions can be studied separately but must be satisfied simultaneously. The left side of Eq. (A.5) is an increasing parabola for $k \geq 0$, and so is equivalent to

$$k < k_{\max} \equiv \left[\left(k_F^2 + k_D^2\right) - \tfrac{1}{4}K^2\sin^2\phi\right]^{1/2} - \tfrac{1}{2}K\cos\phi, \tag{A.6}$$

where $k_{\max}$ is found by requiring the left side of Eq. (A.5) to be zero and choosing the positive solution. The left side of Eq. (A.4) corresponds to a parabola with a minimum at $k = \frac{1}{2}K\cos\phi$. For this value of k the left hand side of Eq. (A.4) becomes $\frac{1}{4}K^2\sin^2\phi - k_F^2$. If $k_F^2 < \frac{1}{4}K^2\sin^2\phi$ Eq. (A.4) is satisfied for all $k \geq 0$; otherwise we must consider the range of k values making the parabola positive. This parabola intersects with the x-axis at the points

$$k_0 \equiv -\left(k_F^2 - \tfrac{1}{4}K^2\sin^2\phi\right)^{1/2} + \tfrac{1}{2}K\cos\phi, \tag{A.7}$$

$$k_{\min} \equiv \left(k_F^2 - \tfrac{1}{4}K^2\sin^2\phi\right)^{1/2} + \tfrac{1}{2}K\cos\phi. \tag{A.8}$$

The intersection point with the y-axis is $K^2/4 - k_F^2$. So if $k_F^2 > K^2/4$ the restriction Eq. (A.4) becomes $k > k_{\min}$; otherwise $k > k_{\min}$ or $k < k_0$. Thus, Eq. (A.4) can be rewritten as

$$\begin{aligned}
&0 < k < \infty && \text{if} \quad k_F^2 < \tfrac{1}{4}K^2\sin^2\phi, \\
&k > k_{\min} && \text{if} \quad k_F^2 > \tfrac{1}{4}K^2\sin^2\phi, \quad \text{and} \quad k_F^2 > \tfrac{1}{4}K^2, \\
&k > k_{\min} \text{ or } k < k_0 && \text{if} \quad k_F^2 > \tfrac{1}{4}K^2\sin^2\phi, \quad \text{and} \quad k_F^2 < \tfrac{1}{4}K^2.
\end{aligned} \tag{A.9}$$

Taking into account that pairs break up for very small CMM (Figs. 2 and 3), we consider only the restriction $k > k_{\min}$, which together with Eq. (A.6) gives

$$k_{\min} < k < k_{\max}, \quad 0 < \phi < \pi/2. \tag{A.10}$$

Note that for larger values of K there exists a minimum value of ϕ below which $k_{\min} > k_{\max}$. Using the dimensionless variables defined below Eq. (18), the $d = 2$ and $d = 3$ expressions for $g(E_F)$ given in the text, and the restrictions Eq. (A.10), one finally obtains Eq. (18) for $d = 2$ and Eq. (21) for $d = 3$.

References

[1] J.R. Schrieffer, Theory of Superconductivity, Benjamin, New York, 1964, p. 33.
[2] J.M. Blatt, Theory of Superconductivity, Academic Press, New York, 1964, and references therein.
[3] L.N. Cooper, Phys. Rev. 104 (1956) 1189.
[4] D.R. Harshman, A.P. Mills, Phys. Rev. B 45 (1992) 10684.
[5] A.L. Fetter, J.D. Walecka, Quantum Theory of Many-Particle Systems, McGraw-Hill, New York, 1971.
[6] P.C. Martin, in: R.D. Parks (Ed.), Superconductivity, vol. 1, Marcel Dekker, New York, 1969.
[7] L. Belkhir, M. Randeria, Phys. Rev. B 49 (1994) 6829.